Smart Structures and Systems, *Vol. 34, No. 2 (2024) 73-85*
https://doi.org/10.12989/sss.2024.34.2.073

Regularized model-free adaptive control of smart base-isolated buildings

Alvaro Javier Florez [1], Luis Felipe Giraldo [2] and Mariantonieta Gutierrez Soto*[3,4]

[1] *Department of Mechanical Engineering, KU Leuven, Celestijnenlaan 300 B-3001 Heverlee, Leuven, Belgium*
[2] *Department of Biomedical Engineering, Universidad de los Andes. Cra. 1#18a-12, Bogotá, Colombia*
[3] *School of Engineering Design and Innovation, The Pennsylvania State University, 307 Engineering Design and Innovation Building, University Park, Pennsylvania, 16802, USA*
[4] *Department of Architectural Engineering, The Pennsylvania State University, 104 Engineering Unit A, University Park, Pennsylvania, 16802, USA*

(*Received August 17, 2022, Revised April 28, 2023, Accepted September 11, 2024*)

Abstract. Smart base-isolated buildings rest on flexible pads known as base isolators that minimize the effect of external disturbances along with active/semi-active actuators. The strategies used to control these active components are typically based on system models that are known a priori. Although these models describe some of the most important dynamics of the elements involved in the system, the high degree of uncertainty in the behavior of a structure under external disturbances is very difficult to characterize using a fixed model. In this work, we propose a strategy that deals with this issue: the input that controls the actuator in the base isolation system results from the compound action of a controller that relies on a model of the system that is known a priori, and a control policy that is designed based on online data-driven inferences on the behavior of the system. In this way, the control design process incorporates both the prior information about the system and the unknowns of the system, such as non-modeled parameters and nonlinear behaviors in the building. We show through simulations the performance of the proposed method in an eight-story building subjected to seismic loading.

Keywords: adaptive control; base-isolated; data-driven; regularized; smart structures; vibration reduction

1. Introduction

Natural hazards continue to challenge the safety and serviceability of the built environment. An earthquake protection system is defined as a system that modifies the dynamic interaction between a building structure and ground motion. These innovative solutions include equipping structures with devices to help protect against worst-case scenarios.

For example, Madhekar and Jangid (2010) used variable dampers installed in highway bridge structures. Jahangiri *et al*. (2021) used pendulum-tuned mass damper for vibration mitigation of offshore wind turbines. Tuned liquid sloshing dampers in tall buildings can help mitigate the vibrations caused by wind loading (Suthar and Jangid 2021). Additional structural control devices have captivated researchers in recent years. Duan *et al*. (2022) studied a viscous inertial mass damper to reduce structural vibrations via energy dissipation, Wang *et al*. (2020) conducted a dynamic analysis of nonlinear energy sinks (Gomez *et al*. 2021), Lotfi *et al*. (2020) proposed a pure torsional yielding damper, Lu (2019) investigated inertial mass dampers, and Downey *et al*. (2019) constructed a cam-based passive variable friction device. Asfaw *et al*. (2022) fabricated a shape memory alloy-based friction damper and experimentally tested its temperature and rate performance.

Semi-active devices offer adaptability in real-time, and to demonstrate the usefulness of semiactive devices Cha *et al*. (2014) studied the performance of a large-scale study of magneto-rheological (MR) damper as an effective strategy for reducing vibrations in building structures subjected to seismic loading. MR dampers are innovative semi-active control devices that control the fluid's properties by tuning the magnetic field (Spencer Jr *et al*. 1997, Kavyashree *et al*. 2021). Huang *et al*. (2015) conducted a full-scale experiment to study the performance of MR dampers installed on cable-stayed bridges. Some important considerations include controlling the gap size for the fluid to travel within the device (Hee *et al*. 2021), numerical modeling characterization (Woo and Lee 2013), effectiveness under uncertainties such as earthquake ground motion and structure-damper properties (Mohebbi and Bakhshinezhad 2021), or sandwich configuration with 1MR elastomers (Yeh 2016).

Base isolation is a widely used technique to prevent damages in civil structures that are underground shaking or wind disturbances as reported in Harvey Jr and Kelly (2016), Warn and Ryan (2012), Sun and Li (2010) and Javadinasab Hormozabad and Gutierrez Soto (2021). Instrumented building and bridge structures equipped with base isolation systems in Japan provided additional insights into understanding dynamic structural performance during earthquake events (Fujino *et al*. 2019, Yunsong *et al*. 2022).

*Corresponding author, Ph.D., Assistant Professor,
E-mail: mvg5899@psu.edu
[a] E-mail: alvaro.florez@kuleuven.be
[b] Ph.D., E-mail: lf.giraldo404@uniandes.edu.co
[c] Ph.D., E-mail: mvg5899@psu.edu

ISSN: 1738-1584 (Print), 1738-1991 (Online)

A building that implements this type of technology rests on flexible pads known as base isolators that minimize the effect of external disturbances. A comparative study of a hospital building with and without base isolation demonstrates its effectiveness in reducing vibrations (Ferj and Lopez-Garcia 2022).

During the last few years, active and semi-active devices have been incorporated into base isolation systems. Efforts have been made to find adequate strategies to control such devices under a variety of scenarios as studied by Florez *et al*. (2017), Wang and Dyke (2013), Shrimali *et al*. (2015), Vu *et al*. (2018) and Florez and Giraldo (2018). Smart base-isolated structures have the potential to enhance the protection of building structures during seismic events because the structure will adapt in real-time to a wider bandwidth of frequencies. When the system is designed as active or semi-active, the dynamic response is controlled using computer algorithms that allow real-time adaptation to the building motion. Narasimhan *et al*. (2006) incorporated smart MR devices into an eight-story base-isolated structure to study control strategies. Gutierrez Soto and Adeli (2018) studied game theoretical control strategies using the benchmark of the smart base-isolated structure to evaluate the performance in mitigating the vibrations caused by earthquake loading. Florez *et al*. (2021) studied structural sparsity to control active and semi-active devices installed in building structures subjected to earthquake loading. Micheli *et al*. (2020) studied high-performance control systems on tall buildings subjected to wind loading.

An adaptive controller is a "controller with adjustable parameters and a mechanism for adjusting the parameters" (Åström and Wittenmark 2013). This ability is particularly useful during unpredictable catastrophic events such as earthquakes. Yu *et al*. (2016) studied a sliding mode control algorithm to reduce the vibrations of a building equipped with base isolation made with a magnetorheological elastomer material. Muthalif *et al*. (2017) use fuzzy logic and proportional-integral-derivative to control the semi-active damping device. Javad *et al*. (2022) investigated multi-feature model predictive control that combines linear programming with a whale optimization algorithm for vibration reduction of tall buildings subjected to earthquake loading. Adaptive control methods have also been used to tackle parameter identification and compensation errors caused during the substructuring of a physical building model (Guo *et al*. 2016). Control algorithms for smart structures and machines can have feedback and feedforward configurations and are subdivided into classical control, optimal control, robust control, and intelligent control (Gutierrez Soto and Adeli 2017). The authors also include innovative controllers that combine energy harvesting and self-powering features. Javadinasab Hormozabad and Gutierrez Soto (2021) reviewed passive, semi-active, and active vibration control methods across civil, electrical, mechanical, and aerospace engineering domains. The authors consider centralized, decentralized, and distributed configurations; and integrated architectures that combine damage-tolerance control with structural health monitoring and energy harvesting.

The methodologies to design control strategies for active and semi-active devices in base isolation systems employ a fixed mathematical model of the structure that characterizes the linear and nonlinear behavior of the structure. Although these models describe some of the most important dynamics of the elements involved in the system, the high degree of uncertainty in the behavior of a structure under external disturbances is very difficult to characterize using a fixed model. There is a need to propose control strategies that consider a model of the structure and incorporate information from the observed dynamics of the system. We do this in this work.

Current research is being conducted to study control design techniques that are driven by online observations of the system's behavior, as opposed to the typical design methods that depend on a system model known *a priori*. These techniques aim to make inferences on unmodeled parameters, complex dynamics, and nonlinear behaviors using the measured data from the plant and conducting an online or off-line data analysis to calculate the control action (Hou and Wang 2013, Tanaskovic *et al*. 2017, Xia *et al*. 2013). Even though data-driven techniques have interesting properties that benefit the control design task, they must be used carefully in systems such as base-isolated buildings. Typically, in this type of system, external disturbances do not occur often. When they do, they can produce fast and unpredictable changes in the system's acceleration that require fast responses from the controller. A control action that depends entirely on data can potentially fail to minimize the damage to the structure mainly in the online strategies when for any time instant the system assumptions do not hold. In this work, we propose a strategy that deals with this issue: the input that controls the base isolation system results from the compound action of a controller that relies on a model of the system that is known *a priori*, and a control policy that is designed based on data-driven inferences on the behavior of the system. Based on the previously proposed Model-Free Adaptive Control (MFAC) method (Hou 2014), we formulate a strategy that is derived from an optimality criterion that has two components to compute the control action: i) a component based on the error between desired and actual outputs, where the predicted response of the system is calculated in an online fashion using concepts such as partial pseudo derivative and dynamic linearization, and ii) a component based on any model-based control output. The first component accounts for non-modeled parameters, nonlinear behaviors in the building materials and actuators, unbalanced loads at each story, the dynamics caused by human-induced vibrations, and dynamic loading from heavy vehicles, among others. The second one incorporates prior information of the system into the control action. We call this strategy Regularized Model-Free Adaptive Control (RMFAC), since the second component can be seen as a regularization term added to an objective function in an optimization problem.

In this paper, the proposed MFAC method to design data-driven controllers is presented for the first time in structural control of smart building structures (Section 2). Then, we introduce the proposed RMFAC method (Section 3), followed by a set of simulations (Section 4) that show the advantages of the RMFAC over other techniques. Validation of the proposed method is shown using a

numerical simulation of an eight-story structure with a base isolation elastomeric bearing device and an actuator connected from the base to the first floor subjected to earthquake loading. Comparison results show that the proposed RMFAC method provides better performance than a strategy that is entirely based on online data inferences or that is designed based on a previously known model, taking the best of both approaches.

2. Model Free Adaptive Control (MFAC)

MFAC is an online technique that only uses the input/output data from the system to compute the control signal. Consider a general multiple inputs - multiple outputs (MIMO) discrete system that is described by Nise (2020)

$$\boldsymbol{y}(k+1) = \mathbf{f}(\boldsymbol{y}(k), \boldsymbol{u}(k)) \tag{1}$$

where $\boldsymbol{y}(k) \in \mathbb{R}^n$ and $\boldsymbol{u}(k) \in \mathbb{R}^m$ are the system's outputs and inputs at time k, and $\mathbf{f}(\cdot)$ is an unknown function. According to Hou (2014), some assumptions on the system in (1) have to be set to have some guarantees on the behavior of the controlled system.

Assumption 1. *The partial derivatives of* $f_i(\cdot), i = 1, \dots, m$ *with respect to each input* $u_i(k)$ *are continuous*.

Assumption 2. *The system described in* (*1*) *satisfies the Lipschitz condition*. *It means that there exists a positive constant* b *such that*

$$\|\boldsymbol{y}(k_1+1) - \boldsymbol{y}(k_2+1)\| \leq b\|\boldsymbol{u}(k_1) - \boldsymbol{u}(k_2)\|$$

Where

$$k_1 \neq k_2 \quad \text{with} \quad k_1, k_2 > 0.$$

According to (Hou 2014, Theorem 3.6), if the system satisfies Assumptions 1 and 2, then there exist a function $\boldsymbol{\Phi}(k) \in \mathbb{R}^{n \times n+m}$ such that the system can be approximated as

$$\boldsymbol{y}(k+1) = \boldsymbol{\Phi}[\boldsymbol{y}(k)\boldsymbol{u}(k)]^T \tag{2}$$

Matrix $\boldsymbol{\Phi}$ is unknown, and it is called the pseudo-system matrix (PSM). If we consider the specific time-variant linear system

$$\boldsymbol{y}(k+1) = \boldsymbol{A}(k)\boldsymbol{y}(k) + \boldsymbol{B}(k)\boldsymbol{u}(k) \tag{3}$$

for all k, the PSM can be expressed as $\boldsymbol{\Phi} = [\boldsymbol{A}(k)\boldsymbol{B}(k)]$. Therefore, the model form of (2) can be considered as the dynamic linearization of a time-variant system.

2.1 Control algorithm

The goal of the MFAC control rule is to find a control signal $\mathbf{u}(k)$ such that the output of the system $\mathbf{y}(k+1)$ follows the desired output $\mathbf{y}^*(k+1)$. In MFAC, finding $\mathbf{u}(k)$ results from minimizing an objective function that uses the approximation in Eq. (2). The cost function is defined as

$$\begin{aligned} J\big(\boldsymbol{u}(k)\big) = &\|y^*(k+1) - y(k+1)\|^2 \\ &+\lambda\|u(k) - u(k-1)\|^2 \end{aligned} \tag{4}$$

where $\boldsymbol{y}^*(k+1)$ is the desired value of the outputs. The first term of the right-hand side of the equation is the error between the desired and actual outputs. The second term of the right-hand side of the equation, whose importance is determined by parameter $\lambda > 0$, penalizes sudden changes in the control signal. The control law requires the real measurement of the output at time $k, \boldsymbol{y}(k)$, and requires an estimation of the PSM denoted as $\hat{\boldsymbol{\Phi}}$. MFAC estimates this matrix by minimizing the cost function $Q(\hat{\boldsymbol{\Phi}})$ which is defined as (Hou 2014, Eq. 5.49)

$$\begin{aligned} Q\big(\hat{\boldsymbol{\Phi}}\big) = &\big\|\boldsymbol{y}(k) - \hat{\boldsymbol{\Phi}}[\boldsymbol{y}(k-1)\boldsymbol{u}(k-1)]^T\big\|_2^2 \\ &+\mu\big\|\hat{\boldsymbol{\Phi}} - \hat{\boldsymbol{\Phi}}_p\big\|_F^2 \end{aligned} \tag{5}$$

where $\hat{\boldsymbol{\Phi}}$ based on the real output $\boldsymbol{y}(k)$ measured at the current time k, and $\hat{\boldsymbol{\Phi}}_p$ is a previous PSM estimation. This function to be minimized corresponds to the squared error between the real output and the estimated one, penalized by a term that enforces slow changes in the PSM matrix. Solving the optimization problems with cost functions (4) and (5), results in an update of the PSM and a computation of the control signal. Note that for the cases when parameters e.g. μ are not well tuned, the updates of PSM can be slow, making the systems susceptible to fail.

3. Regularized Model-Free Adaptive Control (RMFAC)

MFAC is a model-free technique that only uses online data from the system to estimate the control signal. In this paper, we extend the formulation of the MFAC to incorporate the information from a model-based control action to improve the controller's performance in a base-isolated building. The proposed method adds a regularization term to the cost function used in MFAC to compute the control signal, such that the output of the data-driven controller is forced to move to the proximity of the output given by the model-based controller. In this way, the control signal takes into account both prior information on the model of the system and information based on data-driven inferences. This approach is depicted in Figure 1 presented as follows:

Consider a discrete MIMO system that needs to be controlled. The reference signal at time step $k+1$ is $\boldsymbol{y}^*(k+1)$. Let $\boldsymbol{u}_m(k)$ be the control signal at time step k given by any model-based controller, and let $\boldsymbol{y}(k+1)$ be the (data-driven) estimated output. The Regularized Model-Free Adaptive Control (RMFAC) signal $\boldsymbol{u}(k)$ results from solving the cost function

$$\begin{aligned} J\big(u(k)\big) = &\|\boldsymbol{y}^*(k+1) - \boldsymbol{y}(k+1)\|^2 \\ &+\lambda\|\boldsymbol{u}(k) - \boldsymbol{u}(k-1)\|^2 \\ &+\gamma\|\boldsymbol{u}(k) - \boldsymbol{u_m}(k)\|^2 \end{aligned} \tag{6}$$

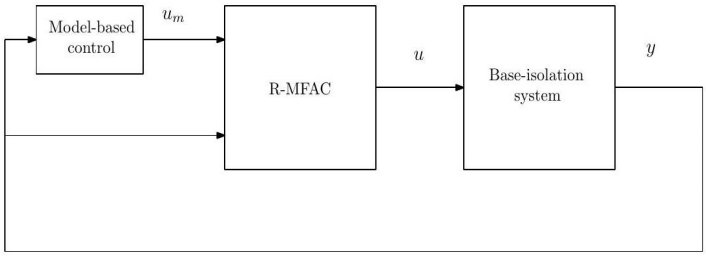

Fig. 1 Diagram that illustrates the controlled-based isolation system using RMFAC. This control strategy takes information from the control signal given by a model-based controller u_m and data-driven inferences based on y to produce an improved control action u

This cost function is based on the error between the desired and actual outputs, a penalization of sudden changes in the control signal, and the error between signal control from data-driven and model-based. Parameter $\gamma \geq 0$ defines the importance of the model-based controller in the design of the control action. When $\gamma = 0$, the control action corresponds to the data-driven policy; when $\gamma \to \infty$, the control action corresponds to the model-based one. To compute $\hat{\boldsymbol{\Phi}}$, we use the same cost function defined in the MFAC method

$$Q(\hat{\boldsymbol{\Phi}}) = \left\|\boldsymbol{y}(k) - \hat{\boldsymbol{\Phi}}[\boldsymbol{y}(k-1)\boldsymbol{u}(k-1)]^T\right\|_2^2 + \mu\left\|\hat{\boldsymbol{\Phi}} - \hat{\boldsymbol{\Phi}}_p\right\|_F^2 \quad (7)$$

Theorem 1 (*Regularized MFAC*). Assume that a discrete MIMO system satisfies Assumptions 1 and 2. The update rules that define the control action that minimizes the cost functions (6) and (7) are

$$\boldsymbol{u}(k) = \left(\hat{\boldsymbol{B}}^T\hat{\boldsymbol{B}} + \lambda + \gamma\right)^{-1}\left(\hat{\boldsymbol{B}}^T\boldsymbol{y}^* - \hat{\boldsymbol{B}}^T\hat{\boldsymbol{A}}^T\boldsymbol{y}(k) + \lambda\boldsymbol{u}(k-1) + \gamma\boldsymbol{u}_m(k)\right) \quad (8)$$

and

$$\hat{\boldsymbol{\Phi}} = \left(\boldsymbol{y}(k)\boldsymbol{z}^T + \mu\boldsymbol{\Phi}_p\right)(\boldsymbol{z}\boldsymbol{z}^T + \mu\boldsymbol{I})^{-1} \quad (9)$$

where $\hat{\boldsymbol{\Phi}} = \left[\hat{\boldsymbol{B}}\hat{\boldsymbol{A}}\right]$, $\boldsymbol{z} = [\boldsymbol{y}(k-1), \boldsymbol{u}(k-1)]^T$, $\boldsymbol{y}^* = \boldsymbol{y}^*(k+1)$ and $\boldsymbol{I}$ is the identity matrix of appropriate dimension.

Proof. The proof has two parts: the derivation of the control law, and the PSM computation. The cost function (6) is a compound function that is the sum of three terms of the form $(\boldsymbol{u}(k)) = J_{u_1} + J_{u_2} + J_{u_3}$. Substituting $\boldsymbol{y}(k+1)$ the simplification of terms are

$$J_{u_1} = \boldsymbol{y}^{T*}\boldsymbol{y}^* - 2\boldsymbol{y}^{T*}[\hat{\boldsymbol{A}}, \hat{\boldsymbol{B}}][\boldsymbol{y}(k), \boldsymbol{u}(k)]^T + [\boldsymbol{y}(k), \boldsymbol{u}(k)]\left[\hat{\boldsymbol{A}}^T, \hat{\boldsymbol{B}}^T\right]^T [\hat{\boldsymbol{A}}, \hat{\boldsymbol{B}}][\boldsymbol{y}(k), \boldsymbol{u}(k)]^T$$

$$J_{u_1} = \boldsymbol{y}^{T*}\boldsymbol{y}^* - 2\boldsymbol{y}^{T*}\hat{\boldsymbol{A}}\boldsymbol{y}(k) - 2\boldsymbol{y}^{T*}\boldsymbol{B}(k)\boldsymbol{u}(k) + \boldsymbol{y}(k)^T\hat{\boldsymbol{A}}^T\hat{\boldsymbol{A}}\boldsymbol{y}(k) + 2\boldsymbol{y}(k)^T\hat{\boldsymbol{A}}^T\hat{\boldsymbol{B}}\boldsymbol{u}(k) + \boldsymbol{u}(k)^T\hat{\boldsymbol{B}}^T\hat{\boldsymbol{B}}\boldsymbol{u}(k)$$

And

$$J_{u_2} = \lambda[\boldsymbol{u}^T(k)\boldsymbol{u}(k) - 2\boldsymbol{u}^T(k)\boldsymbol{u}(k-1) + \boldsymbol{u}^T(k-1)\boldsymbol{u}(k-1)]$$
$$J_{u_3} = \gamma[\boldsymbol{u}^T(k)\boldsymbol{u}(k) - 2\boldsymbol{u}^T(k)\boldsymbol{u}_m(k) + \boldsymbol{u}_m^T(k)\boldsymbol{u}_m(k)]$$

The derivative of $J(\boldsymbol{u}(k))$ with respect to $\boldsymbol{u}(k)$ is

$$\frac{\partial J(\boldsymbol{u}(k))}{\partial \boldsymbol{u}(k)} = -2\left(\boldsymbol{y}^{*T}\hat{\boldsymbol{B}}\right)^T + 2\left(\boldsymbol{y}(k)^T\hat{\boldsymbol{A}}\hat{\boldsymbol{B}}\right)^T + \left(\hat{\boldsymbol{B}}^T\hat{\boldsymbol{B}} + \hat{\boldsymbol{B}}^T\hat{\boldsymbol{B}}\right)\mathbf{u}(k) + 2\lambda\boldsymbol{u}(k) - 2\lambda\boldsymbol{u}(k-1) + 2\gamma\boldsymbol{u}(k) - 2\gamma\boldsymbol{u}_m(k)$$

Simplifying and making zero the expression

$$-2\hat{\boldsymbol{B}}^T\boldsymbol{y}^* + 2\hat{\boldsymbol{B}}^T\hat{\boldsymbol{A}}^T\boldsymbol{y}(k) + 2\hat{\boldsymbol{B}}^T\hat{\boldsymbol{B}}\boldsymbol{u}(k) + 2\lambda\boldsymbol{u}(k) - 2\lambda\boldsymbol{u}(k-1) + 2\gamma\boldsymbol{u}(k) - 2\gamma\boldsymbol{u}(k) = \mathbf{0}$$
$$-\left(\hat{\boldsymbol{B}}^T\hat{\boldsymbol{B}} + \lambda + \gamma\right)\boldsymbol{u}(k) = -\hat{\boldsymbol{B}}^T\boldsymbol{y}^* + \hat{\boldsymbol{B}}^T\hat{\boldsymbol{A}}^T\boldsymbol{y}(k) - \lambda\boldsymbol{u}(k-1) - \gamma\boldsymbol{u}_m(k)$$

$$\boldsymbol{u}(k) = \left(\hat{\boldsymbol{B}}^T\hat{\boldsymbol{B}} + \lambda + \gamma\right)^{-1}\left(\hat{\boldsymbol{B}}^T\boldsymbol{y}^* - \hat{\boldsymbol{B}}^T\hat{\boldsymbol{A}}^T\boldsymbol{y}(k) + \lambda\boldsymbol{u}(k-1) + \gamma\boldsymbol{u}_m(k)\right)$$

In the cost function (7) there are two terms with the form $Q(\hat{\boldsymbol{\Phi}}) = Q_{\Phi_1} + Q_{\Phi_2}$, the simplification of each one is

$$Q_{\Phi_1} = (\boldsymbol{y}(k) - \boldsymbol{\Phi}\boldsymbol{z})^T(\boldsymbol{y}(k) - \boldsymbol{\Phi}\boldsymbol{z})$$
$$Q_{\Phi_1} = \boldsymbol{y}(k)^T\boldsymbol{y}(k) - 2\boldsymbol{y}(k)^T\boldsymbol{\Phi}\boldsymbol{z} + \boldsymbol{z}\boldsymbol{\Phi}^T\boldsymbol{\Phi}\boldsymbol{z}$$

And

$$Q_{\Phi_2} = \mu\left(\mathrm{tr}\left[\left(\hat{\boldsymbol{\Phi}} - \hat{\boldsymbol{\Phi}}_p\right)^T\left(\hat{\boldsymbol{\Phi}} - \hat{\boldsymbol{\Phi}}_p\right)\right]\right)$$
$$Q_{\Phi_2} = \mu\left(\mathrm{tr}\left(\hat{\boldsymbol{\Phi}}^T\hat{\boldsymbol{\Phi}}\right) - \mathrm{tr}\left(\hat{\boldsymbol{\Phi}}^T\hat{\boldsymbol{\Phi}}_p\right) - \mathrm{tr}\left(\hat{\boldsymbol{\Phi}}_p^T\hat{\boldsymbol{\Phi}}\right) + \mathrm{tr}\left(\hat{\boldsymbol{\Phi}}_p^T\hat{\boldsymbol{\Phi}}_p\right)\right)$$

The derivative of the expression with respect to $\hat{\boldsymbol{\Phi}}$ is

$$\frac{\partial Q(\hat{\boldsymbol{\Phi}})}{\partial \hat{\boldsymbol{\Phi}}} = -2\boldsymbol{y}(k)\boldsymbol{z}^T + 2\hat{\Phi}\boldsymbol{z}\boldsymbol{z}^T + 2\mu\left(\hat{\boldsymbol{\Phi}} - \hat{\boldsymbol{\Phi}}_p\right)$$

Making zero the expression and arranging, then we have

$$\hat{\boldsymbol{\Phi}} = \left(\boldsymbol{y}(k)\boldsymbol{z}^T + \mu\hat{\boldsymbol{\Phi}}_p\right)(\boldsymbol{z}\boldsymbol{z}^T + \mu\mathbf{I})^{-1}$$

Note that when $\gamma = 0$ results in the exact close form of pure MFAC methodology. As γ increases, the data-driven control signal $\boldsymbol{u}(k)$ gets to a closer proximity of the solution provided by the modelbased controller $\boldsymbol{u}_m(k)$. Parameter γ can be interpreted as a value that weights the influence of the known model to the data-driven control action. Algorithm 1 summarizes the RMFAC method and 2 shows the flow chart of both methodologies, MFAC and

RMFAC, it allows us to see clearly the differences between them.

4. Simulations

We present numerical simulations to show the performance of the RMFAC method applied to a civil building. We simulate a model of a structure subjected to a seismic loading and compare the control action produced by the MFAC (data-driven), an LQR strategy (model-based policy), and RMFAC (data-driven + model-based) methods in several scenarios.

Algorithm 1 RMFAC

1: Set control of parameters and initial conditions
2: **for** time k **do**
3: Compute $\boldsymbol{u}_m(k)$ from model-based control policy
4: Estimate $\hat{\boldsymbol{\Phi}}$ in Equation (9)
5: Compute $\boldsymbol{u}(k)$ in Equation (8)
6: Observe the system's response $\boldsymbol{y}(k)$
7: **end for**

4.1 Base isolation building model

A base isolation system such as an elastomeric bearing is a flexible device that has elastic and plastic properties that can be represented as an element with hysteresis. It is placed in the base of a structure and works as a passive control mechanism increasing the structure's elasticity. This component has a nonlinear restoring force that can be described by the Bouc-Wen model (Ikhouane and Rodellar 2007) with the following expressions

$$f_b(t) = \alpha\xi x(t) + (1-\alpha)D_b\xi z(t) \tag{10}$$

$$\begin{aligned}\dot{z}(t) = D_b^{-1}(A_b\dot{x}(t) - \beta|\dot{x}(t)||z(t)|^{m_b-1}z(t) \\ - \gamma_b\dot{x}(t)|z(t)|^{m_b})\end{aligned} \tag{11}$$

where $m_b > 1, D_b > 0, \xi > 0, 0 < \alpha < 1, \beta + \gamma_b \neq 0$, are the parameters that rule the behavior of the hysteric cycle. Variable $z(t)$ determines the dependence on preceding device dynamics. Variables $x(t)$ and $\dot{x}(t)$ are the position and velocity of the base isolation device at time t. Base isolator dynamics are transformed to discrete-time using Euler's approximation.

4.2 Mathematical model of the building

Let us consider a n-story building structure. Its model is constructed based on Newton's second law (Chopra 2007), which results in a linear model that depends on $\mathbf{M}, \mathbf{C}$, and $\mathbf{K} \in \mathbb{R}^{n\times n}$, which are the mass [Kg], damping [Ns/m] and stiffness matrices [N/m] (Thenozhi and Yu 2013). The movement equation that represents the n-story building shown in Fig. 3 is presented in Rodellar *et al*. (2017) as

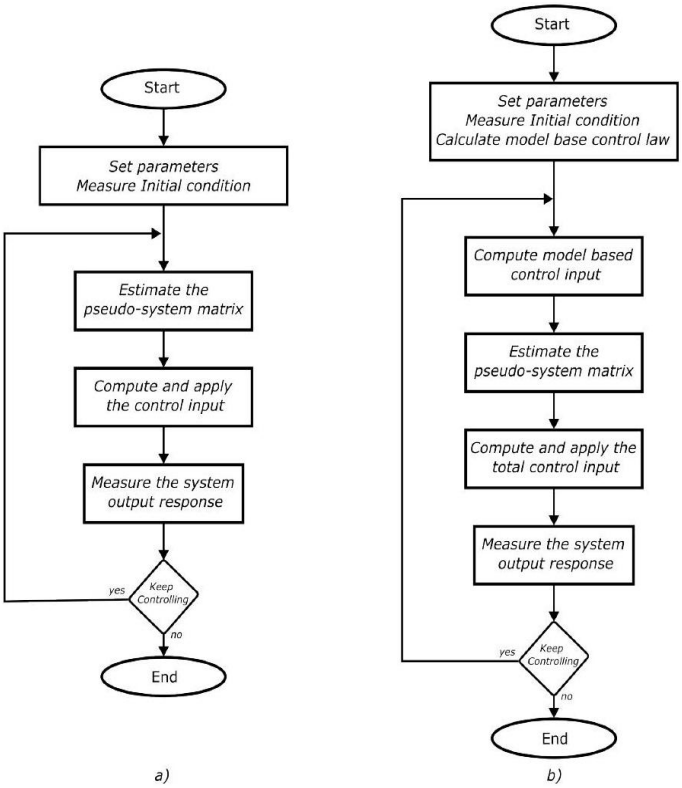

Fig. 2 Flow charts for the MFAC and RMFAC algorithms. Left column (a) shows the MFAC algorithm which can be seen that it is purely data-based. Right column (b) shows the RMFAC approach which uses model information and includes it to improve the controller performance

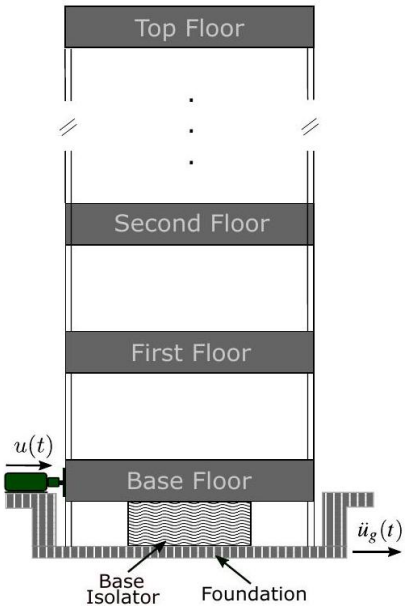

Fig. 3 Diagram on a n-story building equipped with the base-isolation system and semi-active/active devices. The earthquake accelerogram is $\ddot{u}_g(t)$, and signal $u(t)$ is the force exerted by an ideal actuator in the base story

$$\begin{aligned}&\mathbf{M}\ddot{\boldsymbol{x}}(\boldsymbol{t}) + \mathbf{C}\dot{\boldsymbol{x}}(\boldsymbol{t}) + \mathbf{K}\boldsymbol{x}(t)\\&= -\mathbf{M}\Lambda\ddot{u}_g(t) + \Gamma\boldsymbol{u}(t) + \boldsymbol{\Sigma}f_b(t)\end{aligned} \tag{12}$$

where $\boldsymbol{x}(t), \dot{\boldsymbol{x}}(t)$ and $\ddot{\boldsymbol{x}}(t)$, are n-dimensional vectors that correspond to the horizontal position, velocity, and acceleration of the stories. Variable $\ddot{u}_g(t)$ contains the ground accelererogram, $\boldsymbol{u}(t)$ is the control signal, and $f_b(t)$ is the force generated by the base isolation. Parameter $\Lambda \in \mathbb{R}^{n\times 1}$ is the perturbation influence vector, $\Gamma \in \mathbb{R}^{n\times 1}$ is the control system placement vector, $\Sigma \in \mathbb{R}^{n\times 1}$ is the base isolation force placement vector which defines the isolator position (base floor). Vectors above mentioned are defined as

$$\Lambda = [1,1,\dots,1]^T\ \Gamma = [1,0,\dots,0]^T\ \Sigma = [1,0,\dots,0]^T$$

Matrices $\mathbf{M}, \mathbf{C}$, and $\mathbf{K} \in \mathbb{R}^{n\times n}$ have the following form

$$\mathbf{M} = \mathrm{Diag}[m_1, m_2, \dots, m_n]$$

$$\mathbf{C} = \begin{bmatrix} c_1 + c_2 & -c_2 & \cdots & 0 & 0 \\ -c_2 & c_2 + c_3 & \cdots & 0 & 0 \\ \vdots & \vdots & \ddots & \vdots & \vdots \\ 0 & 0 & \cdots & c_{n-1} + c_n & -c_n \\ 0 & 0 & \cdots & -c_n & c_n \end{bmatrix}$$

$$\mathbf{K} = \begin{bmatrix} k_1 + k_2 & -k_2 & \cdots & 0 & 0 \\ -k_2 & k_2 + k_3 & \cdots & 0 & 0 \\ \vdots & \vdots & \ddots & \vdots & \vdots \\ 0 & 0 & \cdots & k_{n-1} + k_n & -c_n \\ 0 & 0 & \cdots & -k_n & k_n \end{bmatrix}$$

where m_i, k_i, c_i are mass, stiffness and damping parameters. Let $\boldsymbol{y}(t) = [\boldsymbol{x}(t), \boldsymbol{v}(t)]^T$ be the state vector where $\boldsymbol{v}(t) = \dot{\boldsymbol{x}}(t)$. Then, Eq. (12) can be rearranged to express the system in a state space form as

$$\begin{aligned}\dot{\boldsymbol{y}}(t) = &\begin{bmatrix} \mathbf{0}_n & \mathbf{I}_n \\ -\mathbf{M}^{-1}\mathbf{K} & -\mathbf{M}^{-1}\mathbf{C} \end{bmatrix}\boldsymbol{y}(t) + \begin{bmatrix} \mathbf{0}_n \\ -\Lambda \end{bmatrix}\ddot{u}_g(t)\\ &+ \begin{bmatrix} \mathbf{0}_n \\ \mathbf{M}^{-1}\Gamma \end{bmatrix}\boldsymbol{u}(t) + \begin{bmatrix} \mathbf{0}_n \\ \mathbf{M}^{-1}\Sigma \end{bmatrix}f_b(t)\end{aligned} \tag{13}$$

that can be written as

$$\dot{\boldsymbol{y}}(t) = \mathbf{A}\boldsymbol{y}(t) + \mathbf{B}\boldsymbol{u}(t) + \mathbf{E}\ddot{u}_g(t) + \mathbf{N}f_b(t)$$

From this set of equations, note that the disturbances given by $\ddot{u}_g$ affect the acceleration of the ground floor. The discrete version of the system model is calculated to obtain a model with the form defined in (3). The discretization process was made using the zero-order hold method. Note that the 2D baseisolated model does not account for torsional effects nor effects from adjacent structures as studied in Matsagar and Jangid (2010).

4.3 LQR control strategy

Remember that the RMFAC method uses information from a model-based control action. In this example, we use a linear feedback control designed using the discrete LQR method. This is a commonly used technique in the control of base-isolated buildings (Thenozhi and Yu 2013, Chang and Spencer 2010, Miyamoto *et al*. 2018). In this case, it is assumed that all states are measurable and that the system has a feedback configuration of the form $\boldsymbol{u}_m(k) = -\mathbf{F}\boldsymbol{x}(k)$. The optimal discrete LQR problem is typically defined as the minimization of the cost function

$$J_{LQR} = \sum_{k=1}^{\infty} [\boldsymbol{y}(k)^T\mathbf{Q}\boldsymbol{y}(k) + \boldsymbol{u}_m(k)^T\mathbf{R}\boldsymbol{u}_m(k)] \tag{14}$$

where $\mathbf{Q}$ and $\mathbf{R}$ are symmetric and positive definite matrices that define a trade-off between performance and control effort. The feedback matrix can be calculated as the infinite horizon solution of the discrete-time Riccati equation. This solution and more detailed information on this problem is presented in (Jannerup and Sørensen 2008, Chapter 5).

4.4 Simulation results

We now define numerical values for the building model and the control parameters. The structure parameters are defined in Table 1 as in (Pujol *et al*. 2011, Table 1). The ground accelerograms used to simulate the seismic loading are the North-South Component from El Centro historical earthquake (Tso and Hsu 1978), the Kobe earthquake, and the Chichi earthquake. The 1995 Kobe (PGA, 0.62 g) and the 1999 Chichi earthquakes (PGA, 0.2 g) are near-field earthquakes, while the 1940 El Centro earthquake (PGA 0.3 g) is far-field, the time history and the frequency spectrum that show the time behavior and the range of frequencies tested are shown in Fig. 4.

The LQR controller, which will produce the model-based control signal $\boldsymbol{u}_m$ in Fig. 1, is designed with the parameters in Table 1 and matrices $\mathbf{Q} = \mathbf{I} * 20 \times 10^6$ and $\mathbf{R} = \mathbf{I} * 1 \times 10^{-6}$. For the base isolator, the parameters were selected to have base isolation forces in a considerable

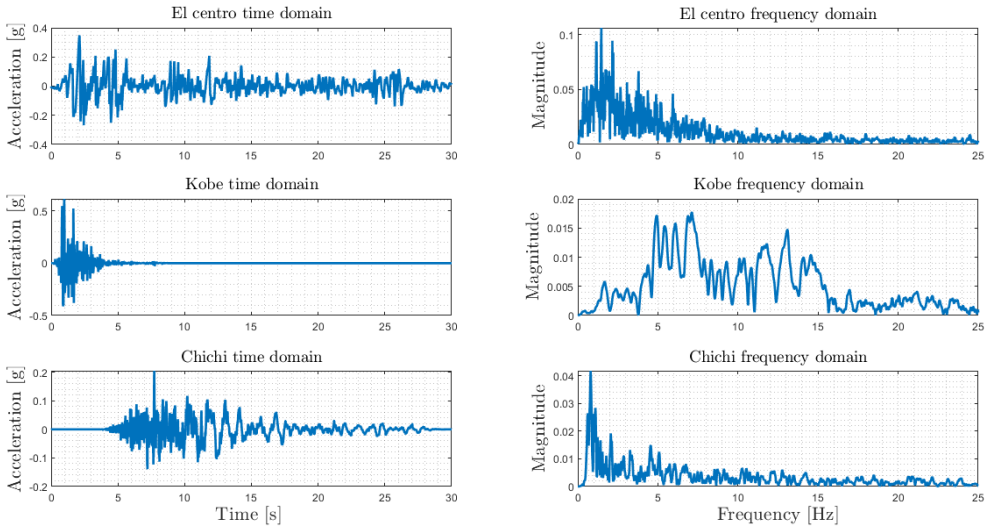

Fig. 4 Accelerograms used to test the controllers. In the left column, the time domain ground accelerograms are applied to the building, In the right column, the frequency spectrum of ground accelerograms applied to the building

Table 1 Structure dynamics parameters of an eight-story building

Story	**Mass** (x1000 **Kg**)	**Stiffness (N/m)**	**Damping (N s/m)**
Base	3565.7	919.422	101439
1st	2580	12913000	11363
2nd	2247	10431000	10213
3rd	2057	7928600	8904
4th	2051	5743900	7578
5th	2051	3292800	5738
6th	2051	1674400	4092
7th	2051	496420	2228
8th	2051	496420	704

range to note its effects in the building and controller parameter values are $A_b = 1, \alpha = 0.5, \xi = 166100,\ D_b = 0.0245, \beta = 0.5, \gamma_b = 0.5, m_b = 1$. The initial value of $\hat{\Phi}$ is defined as the matrices **A** and **B** with the values defined in Eq. (13) and Table 1. Although the RMFAC controller has an adaptive nature, its parameters must be selected so that the controller works in an adequate range of operation. Parameter λ is small to allow fast changes in the control action, μ is large enough to keep $\hat{\boldsymbol{\Phi}} = [\hat{\boldsymbol{A}}, \hat{\boldsymbol{B}}]$ close to the initial values, and γ provides a balance between the data-driven and the model-based control policies. These parameters were selected so that the energy spent by the controller RMFAC is similar to the energy spent by the LQR control policy. The selected values are $\lambda = 1 \times 10^{-18}, \mu = 5 \times 10^{15}$, and $\gamma = 1 \times 10^{-17}$. The model system was discretized with a sampling time of $0.5 \times 10^{-3}[s]$. In this case, the ground accelerograms are linearly interpolated. We tested two versions of the MFAC as a competing algorithm: one that has the same value of lambda as RMFAC (i.e., $= 1 \times 10^{-18}$) that allows fast changes of the control action based on the observed data; and another one, named MFAC2, with a larger value of λ, penalizing the control action such that the result controller spends similar energy as LQR and RMFAC control policies.

We first simulated a scenario where the four controllers (LQR, MFAC, MFAC2 and RMFAC) are tested on the structure with parameters in Table 1, which are the ones that were used to design the LQR controller and to tune the parameters of the data-driven controllers. Then, we simulated a second scenario where the masses of all stories

Table 2 Maximum response for the smart base-isolated structure under control strategies

Earthquake	Response	UC	UC2	LQR	LQR2	MFAC	MFAC2	RMFAC	RMFAC2
El Centro	Displacement (m)	0.22	0.41	0.05	0.16	0.56e − 3	0.22	0.03	0.1
	Acceleration $m/s2$	3.41	3.33	3.43	3.15	3.32	3.45	4.02	3.03
	Actuator Force (MN)	NA	NA	4.64	7.34	13.2	48.5	7.79	9.28
Kobe	Displacement (m)	0.011	0.016	0.007	0.008	0.98e − 3	0.01	0.006	0.008
	Acceleration (m/s^2)	5.51	5.49	5.32	5.47	4.49	5.56	5.3	5.44
	Actuator Force (MN)	NA	NA	2.26	2.02	29.14	100.8	4.3	4.17
Chi Chi	Displacement (m)	0.039	0.024	0.025	0.027	0.25e − 3	0.05	0.013	0.024
	Acceleration (m/s^2)	1.35	1.33	1.49	1.39	1.86	1.39	1.46	1.44
	Actuator Force (MN)	NA	NA	1.62	2.1	9.06	33.22	1.75	3.09

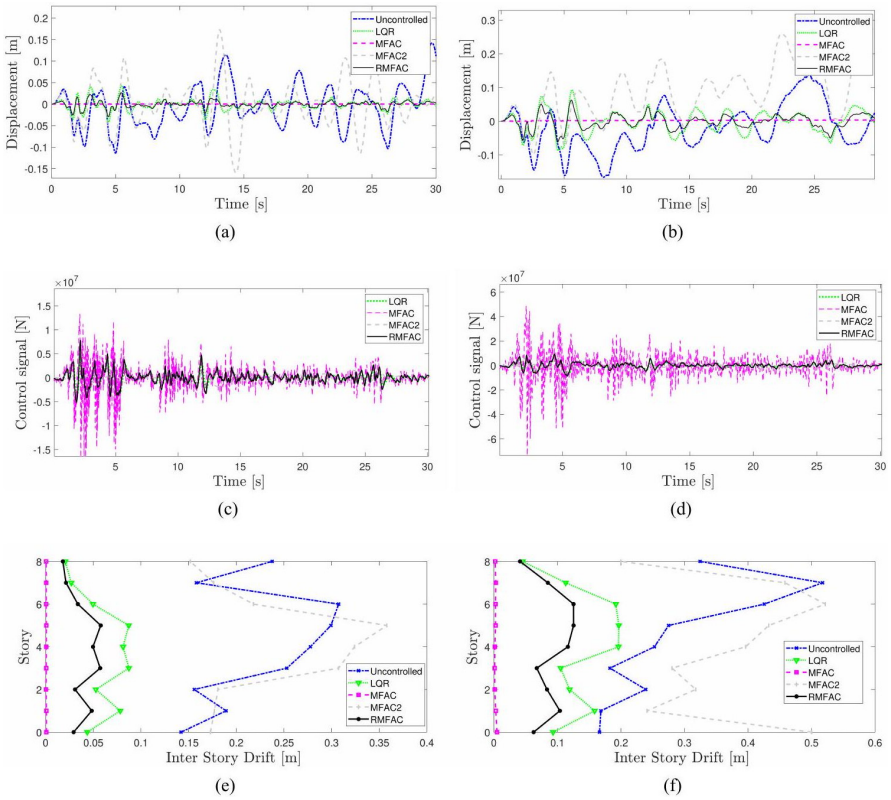

Fig. 5 (a), (b) First-floor displacement; (c), (d) control signals; and (e), (f) inter-story drift between floors during the first thirty seconds of simulation for the uncontrolled system, LQR, MFAC, and the proposed methodology RMFAC when the original structure (left side) and the modified structure (right side) are subjected to El Centro historical earthquake

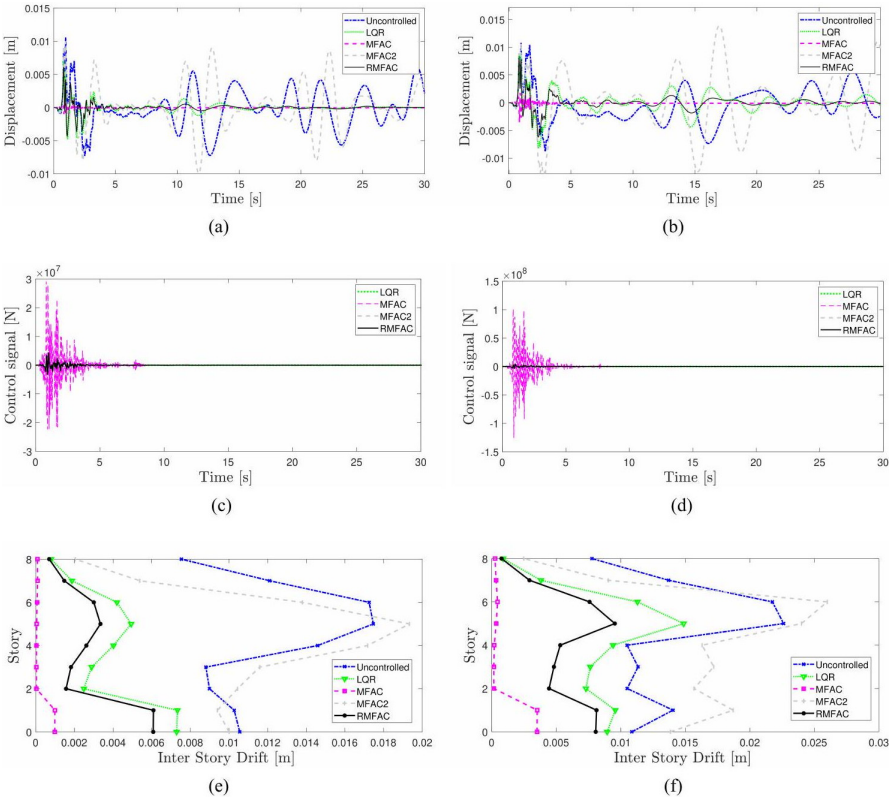

Fig. 6 (a) First-floor displacement; (b) control signals; and (c) inter-story drift between floors during the first thirty seconds of simulation for the uncontrolled system, LQR, MFAC, and the proposed methodology RMFAC when the original structure (left side) and the modified structure (right side) is subjected to historical Kobe earthquake

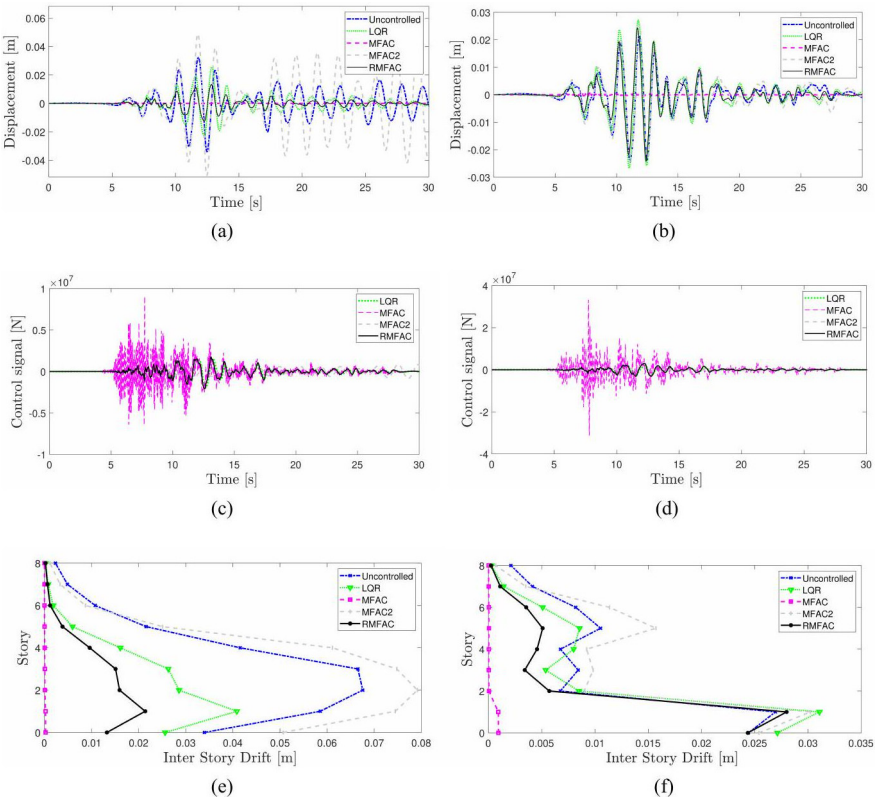

Fig. 7 (a) First-floor displacement; (b) control signals; and (c) inter-story drift between floors during the first thirty seconds of simulation for the uncontrolled system, LQR, MFAC, and the proposed methodology RMFAC when the original structure (left side) and the modified structure (right side) is subjected to historical Chichi earthquake

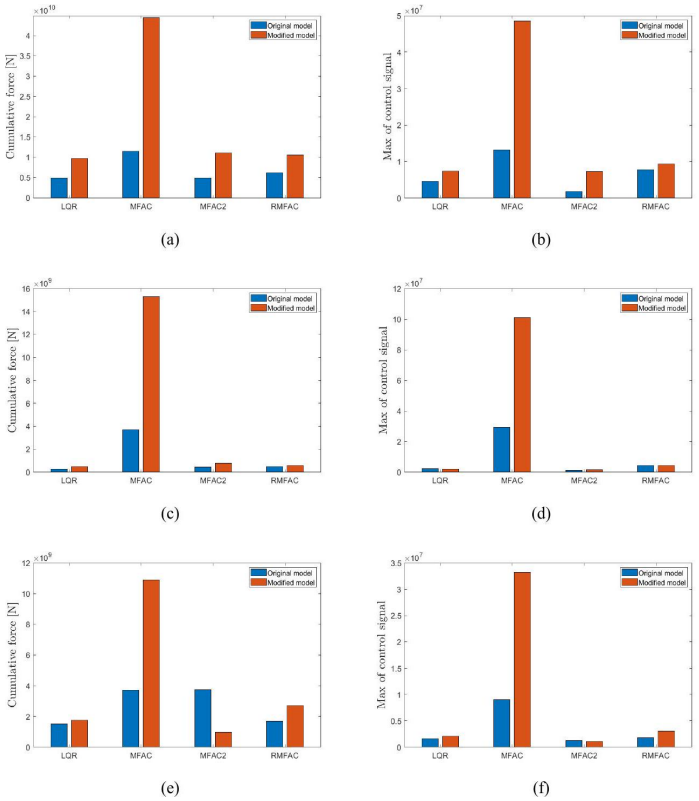

Fig. 8 Left column is the cumulative force exerted by the controller with and without changing model mass parameters, and the right column is the maximum force exerted by the controller with and without changing model mass parameters, both for (a)(b) El Centro; (c)(d) Kobe; (e)(f) Chichi historical earthquakes

were changed by a proportion of: 3.24 for the base; 2.56 for the 1st floor; 1.96 for the 2nd floor; 1.44 for the 3rd floor; 1 for the 4th floor; 1.44 for the 5th floor; 1.96 for the 6th floor; 2.56 for the 7th floor; and 3.24 for the 8th floor. These masses were changed without changing the design of the controllers. In this way, we can study the robustness of the control strategies when the system changes after the control design process. In Fig. 9 we present the plot of system poles and, in table 3 the building natural frequencies to provide a glimpse of the system characteristics in both scenarios. By examining these two elements, we can gain a better understanding of the dynamics of the system and how it will behave under various conditions.

Figs. 5, 6, and 7 show the displacement of the first floor, the control signal, and the interstory drift for each controller for the scenario with the structure in Table 1 and for the scenario with the modified structure. Also, Figure 8 shows the cumulative and the maximum force exerted by the actuator for each controller for each scenario. The cumulative force can be seen as an indirect measurement of the energy used by the actuator.

From these results, note that, in general, MFAC produced the lowest displacement of the first floor and lowest inter-story drift in both scenarios but required a considerable amount of energy to control the structure. This is because it quickly adapts to the vibrating structure. This negatively impacts the feasibility of the implementation of a controller. On the other hand, MFAC2 had the poorest control performance: it spends a similar amount of energy as LQR and RMFAC, but it cannot produce a successful control action based on data. The RMFAC and LQR controllers spent less energy controlling the structure in both scenarios than MFAC. Even though both controllers have similar energy consumption to conduct the control action, RMFAC produces a significantly lower interstory drift than the LQR controller in both scenarios since it adapts according to the system's dynamic behavior and, at the same time, takes into account a policy based on previous information.

The parameter γ which defines the importance of the model-based controller has an important role in the controller performance, therefore, a quantitative analysis is provided. The controller performance is represented by the sum of the maximum inter-story drift. For the cases of the seismic loads considered here, a sweep for parameter γ is shown in Fig. 10. In accordance with the description of RMFAC technique, for small γ values the performance is close to MFAC (black dotted lines), as the γ value increment the performance moves towards the LQR performance (red dashed lines) for all seismic loads. This representation provides a visual quantitative performance and facilitates the interpretation of the γ value selected.

To have an idea of the process that RMFAC conducts to adapt to the seism, we provide an insight into the nonlinear hysteresis force behavior Fig. 11, and we study the evolution of the parameter in $\hat{\boldsymbol{\Phi}}$ associated with the external disturbance. This corresponds to the parameter $\hat{\boldsymbol{B}}$ that affects the displacement of the ground floor in Eq. (13).

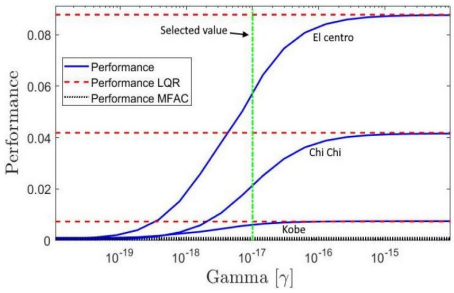

Fig. 10 Performance vs γ value for all seismic loads. Black dotted lines indicate the MFAC performance (close to zero), and red dotted lines show the LQR performance. The vertical green line exhibit the value selected for the above-mentioned results

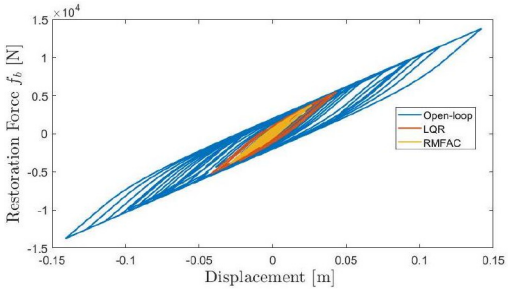

Fig. 11 Nonlinear hysteresis force in the isolation base for El Centro historical earthquake. The relevant control strategies are shown to provide insight into the nonlinear behavior

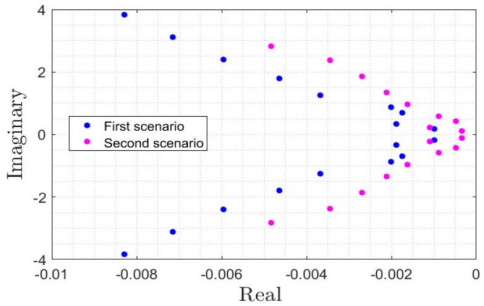

Fig. 9 Poles of the system for the first and second scenario showing that the second scenario has a different configuration

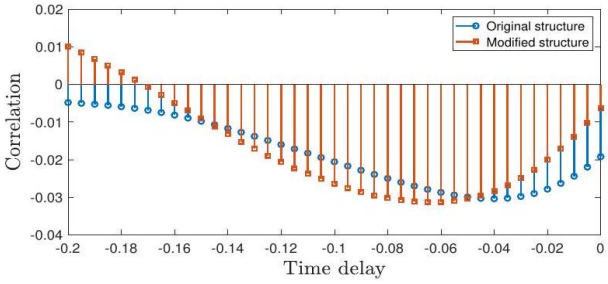

Fig. 12 Cross-correlation between the evolution of the first-floor velocity coefficient and the seism for both scenarios: original structure and modified structure

Fig. 12 shows the cross-correlation between the evolution of this parameter and El Centro, which is an indicator that quantifies the similarity of the signals for a given time delay. The horizontal axis of this plot indicates the time displacement of the parameter evolution with respect to the seism signal. From this plot, we can observe that the maximum correlation occurs at a time lag around 0.05 [s]. This can be interpreted as the RMFAC algorithm taking around 0.05 seconds to adapt to the disturbance that is affecting the structure and to define a control policy accordingly. Given the properties in the frequency domain of El Centro historical earthquake record, this adaptation time seems to be enough to define a control strategy that takes the best of a model-based controller and a data-driven policy.

5. Conclusions

This paper proposed a strategy to design a control input in a smart base-isolated building. The main advantage of this strategy is that it takes information from both a model-based control action and data-driven inferences to design a control signal that incorporates prior information on the system and accounts for unmodeled behaviors of the structure. The strategy presented in this work is formulated using a regularized version of the design criterion in the Model-Free Adaptive Control method. We showed through simulations that the proposed strategy can have a better performance than the model-based controller and is more feasible for practical implementation than the data-driven technique in the proposed scenario. Future research directions include validation of the proposed control method through novel testing technology such as real-time hybrid simulation (Asai *et al*. 2015, Najafi *et al*. 2020, Palacio-Betancur and Gutierrez Soto 2019, Waldbjoern *et al*. 2021), and an extensive analysis of the effect that each design parameter has on the controlled structure. The control algorithms, MFAC and RMFAC, studied in this paper could be promising candidates for challenges in cyber-physical testing highlighted in the comparative study reported by Palacio-Betancur and Gutierrez Soto (2022). Future research is recommended for testing full-scale building structures with base isolation systems as in Brewick *et al*. (2020). On the other hand, Zambrano *et al*. (2021) identifies the vulnerability of smart buildings and bridges to cyber attacks, and mitigation strategies should be a consideration for future studies in structural control.

Acknowledgments

This work was supported by the University of los Andes under Fondo de Apoyo para Profesores Asistentes FAPA.

References

Asai, T., Chang, C.-M. and Spencer Jr, B. (2015), "Real-time hybrid simulation of a smart base-isolated building", *J. Eng. Mech*., **141**(3), 04014128. https://doi.org/10.1061/(ASCE)EM.1943-7889.0000844

Asfaw, A.M., Cao, L., Ozbulut, O.E. and Ricles, J. (2022), "Development of a shape memory alloy-based friction damper and its experimental characterization considering rate and temperature effects", *Eng. Struct*., **273**, 115101. https://doi.org/10.1016/j.engstruct.2022.115101

Åström, K. and Wittenmark, B. (2013), *Adaptive Control*: Second Edition, Dover Books on Electrical Engineering; Dover Publications.

Brewick, P.T., Johnson, E.A., Sato, E. and Sasaki, T. (2020), "Modeling the dynamic behavior of isolation devices in a hybrid base-isolation layer of a full-scale building", *J. Eng. Mech*., **146**(11), 04020127. https://doi.org/10.1061/(ASCE)EM.1943-7889.0001774

Cha, Y.J., Agrawal, A.K., Friedman, A., Phillips, B., Ahn, R., Dong, B., Dyke, S.J., Spencer, B.F., Ricles, J. and Christenson, R. (2014), "Performance validations of semiactive controllers on large-scale momentresisting frame equipped with 200-knmr damper using real-time hybrid simulations", *J. Struct. Eng*., **140**(10), 04014066. https://doi.org/10.1061/(ASCE)ST.1943-541X.0000982

Chang, C.-M. and Spencer, B.F. (2010), "Active base isolation of buildings subjected to seismic excitations", *Earthq. Eng. Struct. Dyn*., **39**(13), 1493-1512. https://doi.org/10.1002/eqe.1040

Chopra, A. (2007), *Dynamics of Structures*: *Theory and Applications to Earthquake Engineering*, Prentice Hall International Series in Civil Engineering and Pearson/Prentice Hall.

Downey, A., Theisen, C., Murphy, H., Anastasi, N. and Laflamme, S. (2019), "Cam-based passive variable friction device for structural control", *Eng. Struct*., **188**, 430-439. https://doi.org/10.1016/j.engstruct.2019.03.032

Duan, Y.F., Dong, S.H., Xu, S.L. and Yun, C.B. (2022), "Optimal design of a viscous inertial mass damper for a taut cable by the fixed-points method", *Smart Struct. Syst*., *Int. J*., **30**(1), 89-106. https://doi.org/10.12989/sss.2022.30.1.089

Ferj, M. and Lopez-Garcia, D. (2022), "Comparative seismic fragility analysis of conventional and base isolated hospital buildings having different structural systems", *J. Earthq. Eng*., **26**(5), 2491-2513. https://doi.org/10.1080/13632469.2020.1767229

Florez, A.J. and Giraldo, L.F. (2018), "Structural sparsity in networked control systems", *IEEE Transact. Syst. Man Cybernet.*: *Syst*., **50**(12), 5152-5161. https://doi.org/10.1109/TSMC.2018.2867187

Florez, A.J., Giraldo, L.F. and Reyes, J.C. (2017), "Structural sparsity for active control design in civil engineering", In: *2017 IEEE Conference on Control Technology and Applications* (*CCTA*), August, Maui, HI, USA, pp. 708-713. https://doi.org/10.1109/CCTA.2017.8062545

Florez, A.J., Giraldo, L.F., Gutierrez Soto, M. and Zuñiga, F.O. (2021), "Structural sparsity in control design of active and semi-active systems", *Struct. Control Health Monitor*., **28**(8), e2758. https://doi.org/10.1002/stc.2758

Fujino, Y., Siringoringo, D.M., Ikeda, Y., Nagayama, T. and Mizutani, T. (2019), "Research and implementations of structural monitoring for bridges and buildings in Japan", *Eng*., **5**(6), 1093-1119. https://doi.org/10.1016/j.eng.2019.09.006

Gomez, F., Fermandois, G.A. and Spencer Jr, B.F. (2021), "Optimal design of nonlinear energy sinks for mitigation of seismic response on structural systems", *Eng. Struct*., **232**, 111756. https://doi.org/10.1016/j.engstruct.2020.111756

Guo, J., Tang, Z., Chen, S. and Li, Z. (2016), "Control strategy for the substructuring testing systems to simulate soil-structure interaction", *Smart Struct. Syst*., *Int. J*., **18**(6), 1169-1188. https://doi.org/10.12989/sss.2016.18.6.1169

Gutierrez Soto, M. and Adeli, H. (2017), "Recent advances in control algorithms for smart structures and machines", *Expert*

Syst., **34**(2), e12205. https://doi.org/10.1111/exsy.12205
Gutierrez Soto, M. and Adeli, H. (2018), "Vibration control of smart base-isolated irregular buildings using neural dynamic optimization model and replicator dynamics", *Eng. Struct*., **156**, 322-336. https://doi.org/10.1016/j.engstruct.2017.09.037
Harvey Jr, P.S. and Kelly, K.C. (2016), "A review of rolling-type seismic isolation: Historical development and future directions", *Eng. Struct*., **125**, 521-531. https://doi.org/10.1016/j.engstruct.2016.07.031
Hee, H., Gon, J., Gu, S. and Hyeok, K. (2021), "Analysis of control performance in gap size of MR damper", *J Korea Inst. Struct. Maint. Inspect*., **25**(1), 41-50. https://doi.org/10.11112/jksmi.2021.25.1.41
Hou, Z. (2014), *Model Free Adaptive Control : Theory and Applications*, CRC Press, Boca Raton, FL, USA.
Hou, Z.-S. and Wang, Z. (2013), "From model-based control to data-driven control: Survey, classification and perspective", *Inform. Sci*., **235**, 3-35. https://doi.org/10.1016/j.ins.2012.07.014
Huang, H., Liu, J. and Sun, L. (2015), "Full-scale experimental verification on the vibration control of stay cable using optimally tuned MR damper", *Smart Struct. Syst*., *Int. J*., **16**(6), 1003-1021. https://doi.org/10.12989/sss.2015.16.6.1003
Ikhouane, F. and Rodellar, J. (2007), *Physical Consistency of the Bouc-Wen Model*, chapter 2, pp. 13-35, Wiley-Blackwell.
Jahangiri, V., Sun, C. and Kong, F. (2021), "Study on a 3d pounding pendulum tmd for mitigating bi-directional vibration of offshore wind turbines", *Eng. Struct*., **241**, 112383. https://doi.org/10.1016/j.engstruct.2021.112383
Jannerup, O. and Sørensen, P.H. (2008), *Linear Systems Control*: *Deterministic and Stochastic Methods*, Springer Berlin Heidelberg: Imprint: Springer, Berlin, Heidelberg, 1st ed. 2008. edition.
Javad, K., Bahrami, R. and Palizvan, Z. (2022), "A novel multi-feature model predictive control framework for seismically excited high-rise buildings", *Struct. Eng. Mech*., *Int. J*., **83**(4), 537-549. https://doi.org/10.12989/sem.2022.83.4.537
Javadinasab Hormozabad, S. and Gutierrez Soto, M. (2021), "Load balancing and neural dynamic model to optimize replicator dynamics controllers for vibration reduction of highway bridge structures", *Eng. Applicat. Artif. Intell*., **99**, 104138. https://doi.org/10.1016/j.engappai.2020.104138
Javadinasab Hormozabad, S., Gutierrez Soto, M. and Adeli, H. (2021), "Integrating structural control, health monitoring, and energy harvesting for smart cities", *Expert Syst*., **38**(8), e12845. https://doi.org/10.1111/exsy.12845
Kavyashree, B.G., Patil, S. and Rao, V.S. (2021), "Comparison of classical and reliable controller performances for seismic response mitigation", *Earthq. Struct*., *Int. J*., **20**(3), 353-364. https://doi.org/10.12989/eas.2021.20.3.353
Lotfi, M., Tajmir, R. and Hashemi, E. (2020), "Investigation on the performance of a new pure torsional yielding damper", *Smart Struct. Syst*., *Int. J*., **25**(5), 515-530. https://doi.org/10.12989/sss.2020.25.5.515
Lu, L. (2019), "Experimental evaluation of an inertial mass damper and its analytical model for cable vibration mitigation", *Smart Struct. Syst*., *Int. J*., **23**(6), 589-613. https://doi.org/10.12989/sss.2019.23.6.589
Madhekar, S. and Jangid, R. (2010), "Seismic response control of benchmark highway bridge using variable dampers", *Smart Struct. Syst*., *Int. J*., **6**(8), 953-974. https://doi.org/10.12989/sss.2010.6.8.953
Matsagar, V. and Jangid, R. (2010), "Impact response of torsionally coupled base-isolated structures", *J. Vib. Control*, **16**(11), 1623-1649. https://doi.org/10.1177/1077546309103271
Micheli, L., Hong, J., Laflamme, S. and Alipour, A. (2020), "Surrogate models for high performance control systems in wind-excited tall buildings", *Appl. Soft Comput*., **90**, 106133. https://doi.org/10.1016/j.asoc.2020.106133
Miyamoto, K., Sato, D. and She, J. (2018), "A new performance index of lqr for combination of passive base isolation and active structural control", *Eng. Struct*., **157**, 280-299. https://doi.org/10.1016/j.engstruct.2017.11.070
Mohebbi, M. and Bakhshinezhad, S. (2021), "Multiple performance criteria-based risk assessment for structures equipped with MR dampers", *Earthq. Struct*., *Int. J*., **20**(5), 495-512. https://doi.org/10.12989/eas.2021.20.5.495
Muthalif, A.G., Kasemi, H.B., Nordin, N.D., Rashid, M. and Razali, M.K.M. (2017), "Semi-active vibration control using experimental model of magnetorheological damper with adaptive F-PID controller", *Smart Struct. Syst*., *Int. J*., **20**(1), 85-97. https://doi.org/10.12989/sss.2017.20.1.085
Najafi, A., Fermandois, G.A. and Spencer Jr, B.F. (2020), "Decoupled model-based real-time hybrid simulation with multi-axial load and boundary condition boxes", *Eng. Struct*., **219**, 110868. https://doi.org/10.1016/j.engstruct.2020.110868
Narasimhan, S.,Nagarajaiah, S., Johnson, E.A. and Gavin, H.P. (2006), "Smart base-isolated benchmark building. part i: problem definition", *Struct. Control Health Monitor*., **13**(2-3), 573-588. https://doi.org/10.1002/stc.99
Nise, N. (2020), *Control Systems Engineering*, Wiley.
Palacio-Betancur, A. and Gutierrez Soto, M. (2019), "Adaptive tracking control for real-time hybrid simulation of structures subjected to seismic loading", *Mech. Syst. Signal Process*., **134**, 106345. https://doi.org/10.1016/j.ymssp.2019.106345
Palacio-Betancur, A. and Gutierrez Soto, M. (2022), "Recent advances in computational methodologies for real-time hybrid simulation of engineering structures", *Arch. Computat. Methods Eng*., **30**, 1637-1662. https://doi.org/10.1007/s11831-022-09848-y
Pujol, G., Acho, L., Pozo, F., Rodriguez, A. and Vidal, Y. (2011), "A velocity based active vibration control of hysteretic systems", *Mech. Syst. Signal Process*., **25**(1), 465-474. https://doi.org/10.1016/j.ymssp.2010.08.011
Rodellar, J., Garcia, G., Vidal, Y., Acho, L. and Pozo, F. (2017), "Hysteresis based vibration control of baseisolated structures", *Procedia Eng*., **199**, 1798-1803. X International Conference on Structural Dynamics.
Shrimali, M., Bharti, S., and Dumne, S. (2015), "Seismic response analysis of coupled building involving mr damper and elastomeric base isolation", *Ain Shams Eng. J*., **6**(2), 457-470. https://doi.org/10.1016/j.asej.2014.12.007
Spencer Jr, B., Dyke, S., Sain, M. and Carlson, J. (1997), "Phenomenological model for magnetorheological dampers", *J. Eng. Mech*., **123**(3), 230-238. https://doi.org/10.1061/(ASCE)0733-9399(1997)123:3(230)
Sun, H. and Li, Q. (2010), "Research and development of seismic base isolation technique for civil engineering structures", In: *2010 International Conference on E-Product E-Service and E-Entertainment*, pp. 1-5.
Suthar, S.J. and Jangid, R.S. (2021), "Design of tuned liquid sloshing dampers using nonlinear constraint optimization for across-wind response control of benchmark tall building", *Structures*, **33**, 2675-2688. https://doi.org/10.1016/j.istruc.2021.05.059
Tanaskovic, M., Fagiano, L., Novara, C. and Morari, M. (2017), "Data-driven control of nonlinear systems: An on-line direct approach", *Automatica*, **75**, 1-10. https://doi.org/10.1016/j.automatica.2016.09.032
Thenozhi, S. and Yu, W. (2013), "Advances in modeling and vibration control of building structures", *Annual Rev. Control*, **37**(2), 346-364. https://doi.org/10.1016/j.arcontrol.2013.09.012
Tso, W. and Hsu, T.-I. (1978), "Torsional spectrum for earthquake motions", *Earthq. Eng. Struct. Dyn*., **6**(4), 375-382.

https://doi.org/10.1002/eqe.4290060405
Vu, D.C., Politopoulos, I. and Diop, S. (2018), "A new semi-active control based on nonlinear inhomogeneous optimal control for mixed base isolation", *Struct. Control Health Monitor.*, **25**(1), e2032. https://doi.org/10.1002/stc.2032
Waldbjoern, J.P., Maghareh, A., Ou, G., Dyke, S.J. and Stang, H. (2021), "Multi-rate real time hybrid simulation operated on a flexible labview real-time platform", *Eng. Struct.*, **239**, 112308. https://doi.org/10.1016/j.engstruct.2021.112308
Wang, Y. and Dyke, S. (2013), "Modal-based lqg for smart base isolation system design in seismic response control", *Struct. Control Health Monitor.*, **20**(5), 753-768. https://doi.org/10.1002/stc.1490
Wang, J., Wang, B., Wierschem, N.E. and Spencer Jr, B.F. (2020), "Dynamic analysis of track nonlinear energy sinks subjected to simple and stochastice excitations", *Earthq. Eng. Struct. Dyn.*, **49**(9), 863-883. https://doi.org/10.1002/eqe.3268
Warn, G.P. and Ryan, K.L. (2012), "A review of seismic isolation for buildings: Historical development and research needs", *Buildings*, **2**(3), 300-325. https://doi.org/10.3390/buildings2030300
Woo, S.S. and Lee, S.H. (2013), "Damping updating of a building structure installed with an MR damper", *Smart Struct. Syst., Int. J.*, **12**(6), 695-705. https://doi.org/10.12989/sss.2013.12.6.695
Xia, Y., Xie, W., Liu, B. and Wang, X. (2013), "Data-driven predictive control for networked control systems", *Inform. Sci.*, **235**, 45-54. https://doi.org/10.1016/j.ins.2012.01.047
Yeh, J.-Y. (2016), "Vibration characteristic analysis of sandwich cylindrical shells with mr elastomer", *Smart Struct. Syst., Int. J.*, **18**(2), 233-247. https://doi.org/10.12989/sss.2016.18.2.233
Yu, Y., Royel, S., Li, J., Li, Y. and Ha, Q. (2016), "Magnetorheological elastomer base isolator for earthquake response mitigation on building structures: modeling and second-order sliding mode control", *Earthq. Struct., Int. J.*, **11**(6), 943-966. https://doi.org/10.12989/eas.2016.11.6.943
Yunsong, X., Siringoringo, D.M. and Fujino, Y. (2022), "Condition assessment of seismically isolated multispan highway bridge bearings using recorded and simulated seismic responses", *Adv. Struct. Eng.*, **25**(16), 3299-3315. https://doi.org/10.1177/13694332221133195
Zambrano, A., Betancur, A.P., Burbano, L., Niño, A.F., Giraldo, L.F., Soto, M.G., Gutierrez Soto, J. and Cardenas, A.A. (2021), "You make me tremble: A first look at attacks against structural control systems", *Proceedings of the 2021 ACM SIGSAC Conference on Computer and Communications Security*, pp. 1320-1337.